15

Study of light propagation in the regime of whispering gallery modes in a cylindrical microresonator with a partially removed silica cladding by hydrofluoric acid etching

© N.A. Makarova[1], V.S. Terentyev[2], I.D. Vatnik[1]

[1] Novosibirsk State University,
630090 Novosibirsk, Russia
[2] Institute of Automation and Electrometry, Siberian BranchRussian Academy of Sciences,
630090 Novosibirsk, Russia

e-mail: n.makarova@g.nsu.ru

Received December 15, 2023
Revised December 21, 2023
Accepted January 29, 2023

We study parameters of cylindrical microresonators based on optical fiber with a partially removed silica cladding by etching with hydrofluoric acid. It was found that a higher degree of silica cladding removal results in a decrease in the quality factor of the microresonator, attributed to the increase in surface roughness.

Keywords: cylindrical microresonator, whispering gallery modes, Q-factor, silica cladding, chemical etching.

DOI: 10.61011/EOS.2024.02.58451.5821-23

Introduction

One of the main elements in many optical devices is a resonator. Microresonator of whispering gallery modes (WGM) have multiple advantages (extreme sensitivity to changes in the refraction index of the environment [1], low effective field volume, high Q-factor [2]), which makes it possible to use them as optical delay lines [3], biosensors [4], devices to study the non-linear effects [5], and in the future — as an element of a quantum supercomputer [6].

One of the promising types of microresonators is a cylindrical microresonator based on quartz optical fibers. The quality of the surface of the silica cladding (SC) of even the regular telecommunications fiber is quite high to maintain the whispering gallery modes with Q factor of at least 10^6 [7]. Besides, the variation of effective radius may precisely control the structure of the modes [8]. For example, for the parabolic form of the effective radius variation, an equidistant spectrum of modes will be observed with various number of maxima along the cylinder axis [9].

In the cylindrical microresonator based on optic fiber the light in the WGM mode spreads inside the quartz shell near its surface, but does not reach the optic fiber core. As the (SC) withdraws, the light in the WGM mode may potentially spread in the optic fiber core material as well. If the radius of the core is $> 10\,\mu$m, the radiation-induced losses will be quite low [10]. Then, if the core is alloyed with a rare earth element, potentially the laser generation may be obtained in such microresonator. In addition, directly in process of making a rare-earth-doped silica cylinder by the method of deposition from the gas phase, alloying may be absent at depth up to several units of microns due to diffusion of active admixtures, i.e. to excite the WGM in the active medium, some surface will have to be removed. Besides, in case of substantial variation of the effective radius, it is possible to significantly vary the dispersion of the cylindrical microresonator, which is necessary to achieve the parametric generation and generation of optical frequency combs in such systems [11].

To change the dispersion and create the laser generation in the microresonator, the objective is to remove the optic fiber SC. One of the known methods to remove the optic fiber SC is the etching method using hydrofluoric acid [12]. It is necessary to note that since the light in WGM mode circulates near the surface, the properties of the modified surface provide noticeable effect on the properties of modes, in particular, their Q factor. Therefore, when removing the SC, it is important to maintain smoothness and homogeneity of the microresonator surface. The irregularities produced on the microresonator surface with the partially removed SC may significantly reduce the microresonator Q factor.

This paper is dedicated to study of the microresonator parameters (Q factor and variation of the effective radius), modified by the etching method using hydrofluoric acid.

Theory

In an optical resonator WGMs arise, when the light due to complete internal reflection, having revolved along the inner surface, returns to the start of its optical path. Due to multiple reflection from the surface of the resonator and the structural interference, only certain wavelengths are excited that comply with the equation

$$2\pi Rn = m\lambda, \tag{1}$$

where m — integer number being the number of the azimuthal mode, i.e. the number of wavelengths within the perimeter; λ — resonant wavelength; R — microresonator radius; n — refraction index of the medium. Further instead of the product Rn we will write the effective radius — r_{ef}. Let us make a certain variation Δr_{ef} of the effective radius in the microresonator, then the resonant wavelength based on the equation (1), will shift by the value of $\Delta\lambda$:

$$\Delta\lambda/\lambda = \Delta r_{ef}/r_{ef}, \tag{2}$$

Therefore, the measurement of the resonance wavelength shift $\Delta\lambda(z)$ along the axis of the cylindrical microresonator z makes it possible to determine the variation $\Delta r_{ef}(z)$ of the effective radius in this point.

Another important parameter, which determines the quality of the microresonator, is Q factor. The Q factor value depends on various types of losses. Appearance of irregularities on the surface results in appearance of additional radiation-induced losses as the light propagates in the WGM mode. For the spherical microresonator the paper [13] demonstrated that Q factor because of surface irregularities was defined as

$$Q \sim \frac{a}{B^2\sigma^2}, \tag{3}$$

where a — radius of spherical microresonator, B determines the specific size of irregularities and is called the correlation length, $\sigma^2 = \langle f(x,z)^2 \rangle$ — mean square roughness of the surface.

From the formula (3) it is seen that Q factor strongly depends on the size of irregularities on the fiber surface. Thus, for $B = 10$ nm and $\sigma = 1$ nm under radiation with wavelength $1.5\,\mu$m in the optical fiber with radius $50\,\mu$m Q factor will be around $10^5 - 10^6$, and if σ is increased 10 times, Q factor will decrease 100 times, i.e. will be $10^3 - 10^4$. Therefore, any appearance of irregularities may substantially worsen Q factor.

Etching velocity measurement

In process of etching the optic fiber with the previously removed protective acrylate cladding was submerged into a vessel with hydrofluoric acid with concentration of 12.5% for a certain time at room temperature. SC was removed partially from the surface of the optic fiber when exposed to HF. Further the etched fiber was washed with distilled water to remove the acid residues on the surface and annealed with heating by focused radiation of CO_2-laser for removal of water from the sample surface. This process was repeated many times to understand the dependence of the SC etching depth (difference between the initial diameter of optic fiber ($125\,\mu$m) and diameter of the fiber after etching) on the etching time (Fig. 1). The velocity of etching was 4.3 nm/s, which is 11 times more than the velocity of etching of the same fiber in 12% HF acid obtained in [14]. The difference in the velocity may be explained by the fact that the time of etching in the paper [14] was in the range of 5-25 s, while in our paper — 15-300 min.

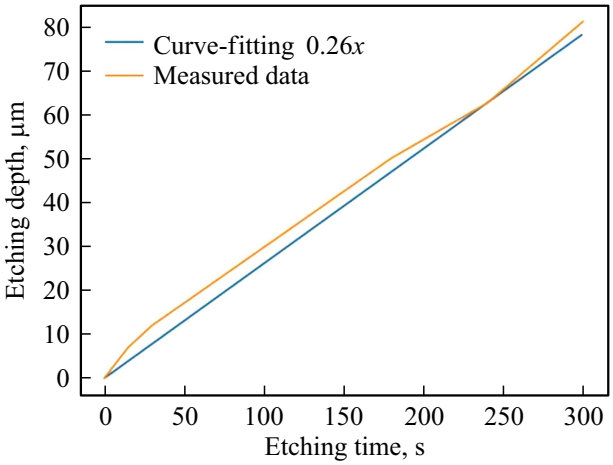

Figure 1. Velocity of SC etching with HF acid with concentration of 12.5%.

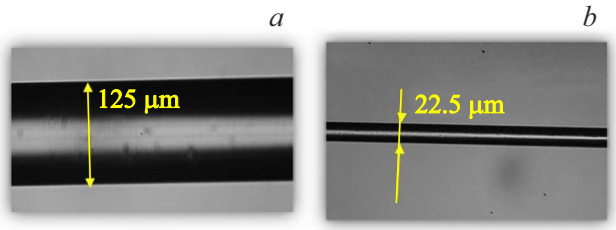

Figure 2. The sample with SC partially removed by etching method using HF: (a) before etching, (b) after etching.

To study the quality of the surface after etching, the sample micrographs were studied (Fig. 2). The surface after etching looks smooth and homogeneous, which makes it possible to suggest the possibility of WGM excitation, the spectra of which will be studied further.

The scheme of the unit for measurement of microresonator parameters

To study the parameters of microresonators, the unit shown in Fig. 3 was used. Biconical fiber 2 is connected to the source of radiation 1 with one end (blue fiber in Fig. 3). This fiber is installed on the platform 3, which may move using moving pads 4 along the sample 5. The spectrum is recorded on the detector 6. Excitation of WGM in the studied sample is carried out by bringing the biconical fiber into the direct contact with the sample. Biconical fiber in this case is located perpendicularly to the axis of the sample, touching it with its waist 7. Due to the evenly narrowing biconical shape of the fiber, the radiation passing along it will experience the effect of the disturbed full internal reflection and partially leak into the studied sample, exciting the WGM in the resonant wavelengths.

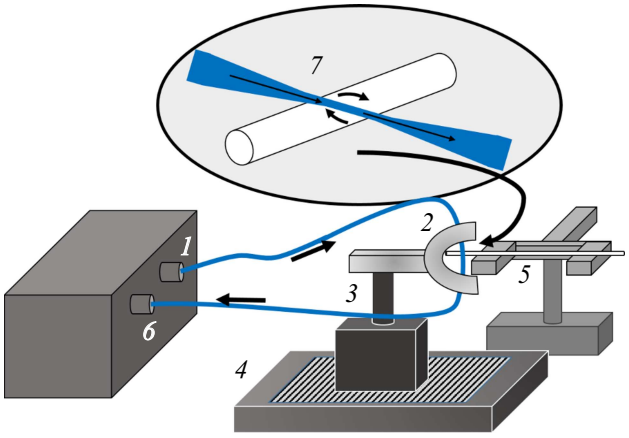

Figure 3. The unit for measurement of the microresonator transmission spectra: *1* — source of radiation, *2* — biconical fiber, *3* — microfiber holder, *4* — moving pad, *5* — sample, *6* — detector, *7* — area of contact of biconical fiber and sample.

Then the radiation, having made several passages in the resonator and suffered losses, returns to the biconical fiber through the contact area. The spectra of transmission of such system demonstrate the minima of intensity at resonant wavelengths located at the spectral distance $\Delta\lambda$ from each other, corresponding with the equation (1) for different m [15]. By the shift of the minimum in the spectrum one may calculate the variation of the effective radius. In process of scanning the biconical fiber moves along the sample, thus exciting the WGM in different points of the resonator [16]. Therefore, the spectrogram is built — dependence of the transmission spectrum and resonance wavelength with the specified azimuthal, radial and polarization numbers on the coordinate of the sample, i.e. the type of the sample modification profile is recorded.

WGM spectra

First the properties of microresonators were studied on the non-modified fiber (type SMF-28). A typical example of the spectrogram is shown in Fig. 4. As one can see, the resonances shift in the spectrum as the exciting biconical fiber moves along the axis of the sample, i.e. there is a non-zero variation of the radius (on the right scale, Fig. 4), arising during fiber production [17]. Q factor in a certain point of the microresonator is determined by measurement of the width at half maximum of WGM resonance. Q factor of the microresonator on the basis of the standard fiber SMF-28, not subjected to etching, is $10^6 - 10^7$ (depending on the point of resonance measurement).

In process of etching the structure of the microresonator surface changes, which results in the change of light propagation in the WGM mode in the modified fiber. At low depths of etching an unnoticeable change in the microresonator Q factor is observed. If etching depth was $14\,\mu$m, the microresonator Q factor was $(1.3 - 3.1) \cdot 10^6$ (depending on the point of resonance measurement), and before etching Q factor was $(1.3 - 5) \cdot 10^6$. Besides, the overall picture of the mode localization along the microresonator axis differs from the spectrogram of transmission of the non-modified fiber. A dispersion of effective radius variations (ERV) appears in the areas of around 0.5 mm along the microresonator axis (shown by arrows in Fig. 5). In the samples with the low etching depth (up to $14\,\mu$m) the dispersion of effective radius variation $\delta\Delta r_{\text{ef}}$ was units of nanometers.

As the etching depth increases, Q factor decreases. Thus, in the sample with etching depth $62\,\mu$m Q factor is $(2.1 - 3) \cdot 10^5$, which is by an order less than in the sample with etching depth $14\,\mu$m. Besides, at the length of around 0.4 mm along the microresonator axis the ERV dispersion increased by several nanometers (Fig. 6). In the samples with higher etching depths Q factor will also continue decreasing (Fig. 7, *a*). Q factor in the sample with etching depth $102.5\,\mu$m made $(1 - 1.2) \cdot 10^4$, i.e. dropped by almost two orders compared to Q factor in the microresonator with etching depth $14\,\mu$m.

As the etching time increases, apart from worsening Q factor, the sample ERV dispersion increases, which is observed at the scale of fractions of millimeters. Such scales are much more than the specific dimensions of the reciprocal value of the wave vector axial component directed along the fiber axis ($\frac{1}{k_z} \sim 50\,\mu$m [18]), i.e. have no effect whatsoever on the Q factor of microresonator modes. Nevertheless, it may be assumed that the increase of ERV dispersion at these scales correlates with increase of mean square roughness of the surface at small scales.

The assumption that the ERV dispersion at large scales and roughness at small scales increase in the same manner makes it possible to describe the Q factor decrease in the experiment. Indeed, in the microresonator with etching depth to $14\,\mu$m the ERV dispersion is $1 - 12$ nm at length of 0.5 mm. Based on the formula (3), as the mean square roughness of the surface increases 3.3 times, Q factor of the microresonator will drop by an order. Such dependence is observed in the experiment: as the etching depth increases to $80\,\mu$m the ERV dispersion increases to 20 nm, and Q factor at the same time reduces approximately by an order. Finally, in the sample with the etching depth $102.5\,\mu$m the ERV dispersion was $50 - 90\,\mu$m, and Q factor decreased by two orders in respect to Q factor of the microresonator with etching depth to $14\,\mu$m (Fig. 7). From the arguments it follows that the longer is the time of acid exposure, the higher is the roughness of the microresonator surface. The effect of roughness increase was previously described both for etching of the quartz glass surface by HF vapors [19] and for etching with liquid phase [20–22].

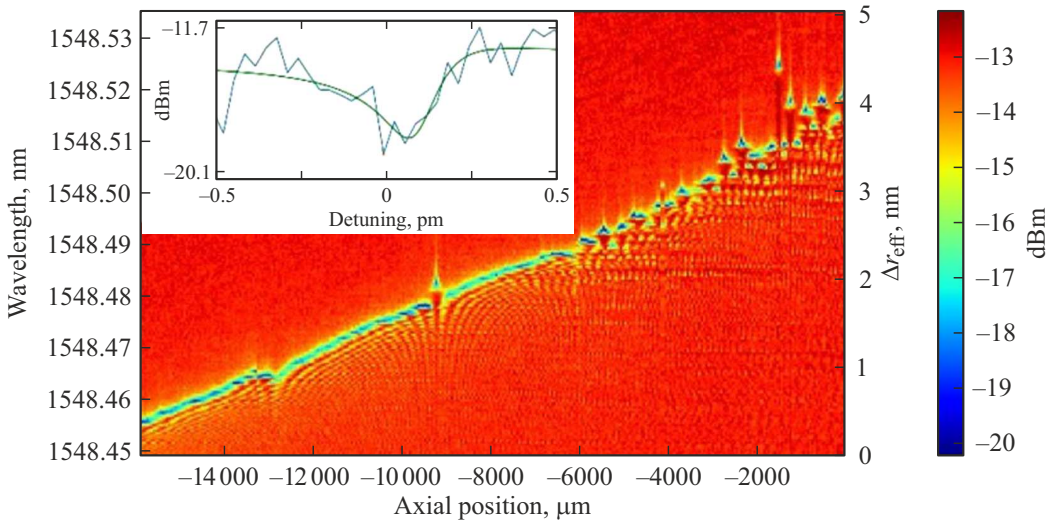

Figure 4. Spectrogram of transmission of the non-modified fiber. SC radius — 62.5 μm. Insert — spectrum of transmission, corresponding to a separate resonanxe with width of 0.25 pm and Q factor $6.2 \cdot 10^6$.

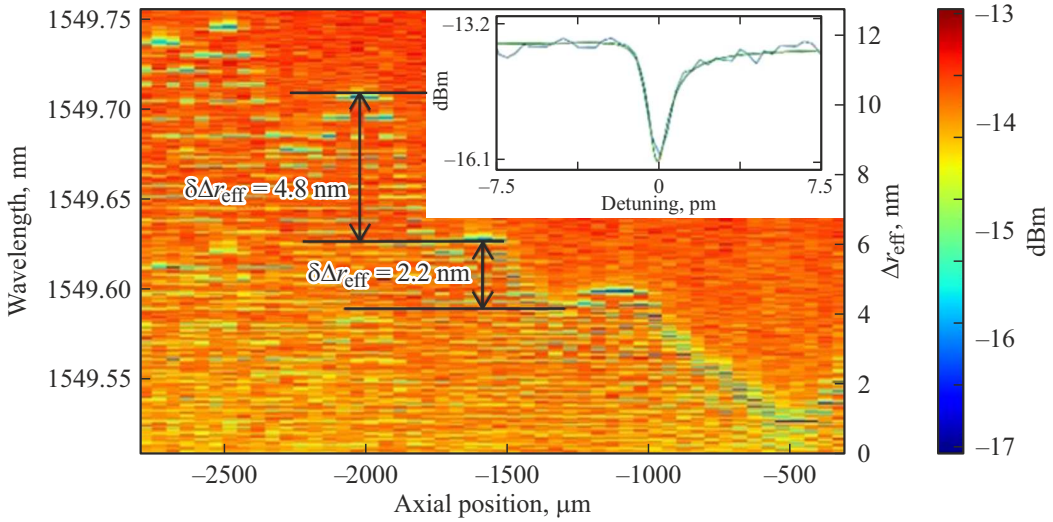

Figure 5. Spectrogram of the sample with etching depth 14 μm. Insert — spectrum of transmission, corresponding to a separate resonanxe with width of 1.32 pm and Q factor $1.2 \cdot 10^6$.

Conclusion

It is shown that WGMs are excited in the samples with the partially removed SC by the etching method using HF. In the samples with the low etching depth (up to 14 μm) the WGMs are excited with Q factor of at least 10^6, which is of the same order as Q factor in the sample with the intact SC. As the depth of etching increased, Q factor of the microresonator decreased as a result of roughness growth on the surface sample. For example, in the samples with etching depth 50–65 μm Q factor was 10^5, which is by an order less than in the cylindrical microresonator with the solid SC. In the sample with the highest obtained etching depth 102.5 μm the light propagation in the WGM mode was also studied. Q factor of the sample was $(1 - 1.2) \cdot 10^4$, which is by two orders less than in the cylindrical microresonator with the solid SC.

As the etching depth increased, the ERV dispersion grew. In the samples with low etching depth (up to 14 μm) the ERV dispersion was units of nanometers, and in the samples with higher etching depth this value increased to tens of nanometers.

Acknowledgments

The paper of V.S. Terentyev was written within the state assignment of the Institute of Automatics and Electrometry of the Siberian Branch of the Russian Academy of Sciences „Development of elements and study of characteristics of laser and sensor systems based on structured wave light

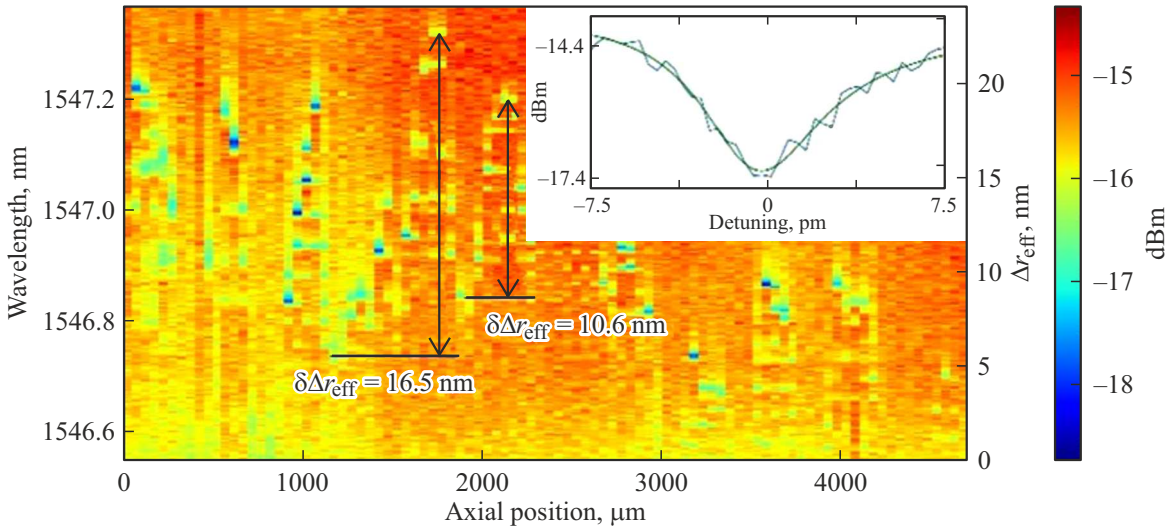

Figure 6. Spectrogram of the sample with etching depth 62.5 μm. Insert - spectrum of transmission, corresponding to a separate resonanxe with width of 7.19 pm and Q factor $2.2 \cdot 10^5$.

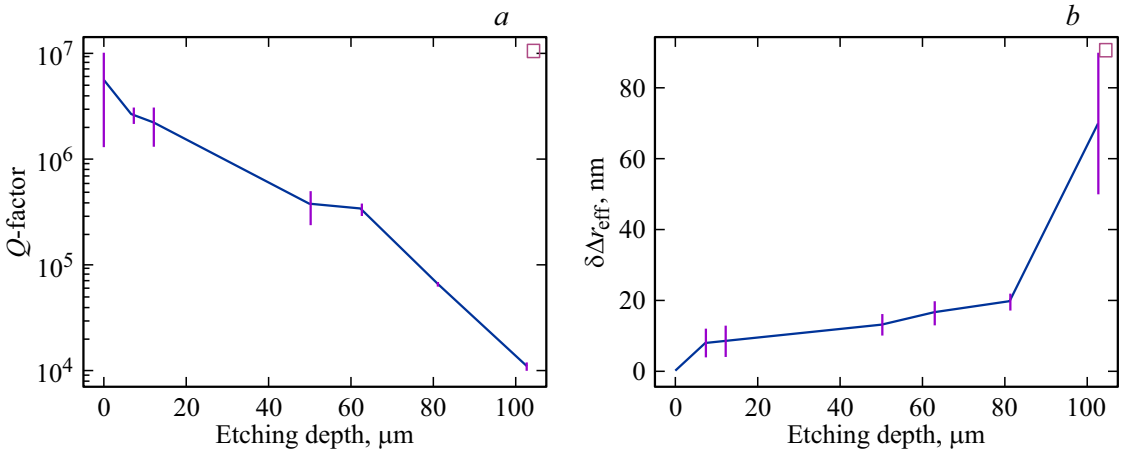

Figure 7. (*a*) Dependence of Q factor of microresonator resonances on the etching depth (vertical sections show the range of Q factor values depending on the point of the microresonator). (*b*) Dependence of the average dispersion of ERV on the etching depth (vertical sections specify the ERV dispersion range depending on the microresonator point)

guides, microresonators and hybrid schemes“ (FWNG-2024-0015). The paper of N.A. Makarova and I.D. Vatnik was supported by the Ministry of Science and Higher Education of the Russian Federation (FSUS-2020-0034).

Conflict of interest

The authors declare that they have no conflict of interest.

References

[1] Y. Zheng, Z. Wu, P. Ping Shum, Z. Xu, G. Keiser, G. Humbert, H. Zhang, S. Zeng, X. Quyen Dinh. Opto-Electronic Advances, **1** (9), 18001501-18001510 (2018). DOI: 10.29026/oea.2018.180015

[2] M. Pöllinger, A. Rauschenbeutel. Opt. Express, **18** (17), 17764–17775 (2010). DOI: 10.1364/OE.18.017764

[3] M. Sumetsky. Phys. Rev. Lett., **111** (16), 163901 (2013). DOI: 10.1103/PhysRevLett.111.163901

[4] Y. Zhang, T. Zhou, B. Han, A. Zhang, Y. Zhao. Nanoscale, **10** (29), 13832–13856 (2018). DOI: 10.1039/C8NR03709D

[5] D. O'Shea, C. Junge, M. Pöllinger, A. Vogler, A. Rauschenbeutel. Appl. Phys. B, **105** (1), 129 (2011). DOI: 10.1007/s00340-011-4714-x

[6] Y.-F. Xiao, Z.-F. Han, G.-C. Guo. Phys. Rev. A, **73** (5), 052324 (2006). DOI: 10.1103/PhysRevA.73.052324

[7] V. Vassiliev, M. Sumetsky. Light Sci. Appl., **12** (1), 197 (2023). DOI: 10.1038/s41377-023-01247-7

[8] M. Sumetsky, Y. Dulashko. Opt. Express, **20** (25), 27896–27901 (2012). DOI: 10.1364/OE.20.027896

[9] M. Crespo-Ballesteros, A.B. Matsko, M. Sumetsky. Commun. Phys., **6** (1), 52(2023). DOI: 10.1038/s42005-023-01168-2

[10] V.B. Braginsky, M.L. Gorodetsky, V.S. Ilchenko. Phys. Lett. A, **137** (7–8), 393–397 (1989). DOI: 10.1016/0375-9601(89)90912-2

[11] V. Dvoyrin, M. Sumetsky. Opt. Lett., **41** (23), 5547–5550 (2016). DOI: 10.1364/OL.41.005547
[12] J.-P. Laine, B.E. Little, H.A. Haus. IEEE Photon. Technol. Lett., **11** (11), 1429–1430 (1999). DOI: 10.1109/68.803068
[13] M.L. Gorodetskiy. *Osnovy teorii opticheskikh mikrorezonatorov* (Fizmatlit, M., 2010), p. 164–166. (in Russian)
[14] N. Toropov, S. Zaki, T. Vartanyan, M. Sumetsky. Opt. Lett., **46** (7), 1784 (2021). DOI: 10.1364/OL.421104
[15] A. Yariv. Electron. Lett., **36** (4), 321 (2000). DOI: 10.1049/el:20000340
[16] T.A. Birks, J.C. Knight, T.E. Dimmick. IEEE Photon. Technol. Lett., **12** (2), 182–183 (2000). DOI: 10.1109/68.823510
[17] M. Sumetsky, Y. Dulashko. Opt. Lett., **35** (23), 4006 (2010). DOI: 10.1364/OL.35.004006
[18] M. Sumetsky. Opt. Express, **20** (20), 22537 (2012). DOI: 10.1364/OE.20.022537
[19] L. Wang, L. Li, Y. Liu, S. Wang, H. Cai, H. Jin, Q. Tang, W. Sun, D. Yang. R. Soc. Open Sci., **7** (7), 192029 (2020). DOI: 10.1098/rsos.192029
[20] J.K. Vondeling. J. Mater. Sci., **18** (1), 304–314 (1983). DOI: 10.1007/BF00543840
[21] C. Mazzitelli, M. Ferrari, M. Toledano, E. Osorio, F. Monticelli, R. Osorio. J. Dent. Res., **87** (2), 186–190 (2008). DOI: 10.1177/154405910808700204
[22] G.A.C.M. Spierings. J. Mater. Sci., **28** (23), 6261–6273 (1993). DOI: 10.1007/BF01352182

Translated by M.Verenikina